Laboratory studies of the rapid densification of oil sands mature fine tailings by microbial activity

Chengmai Guo
Suncor Energy Inc, Fort McMurray, Alberta
Rick J. Chalaturnyk, J. Don Scott,
Department of Civil and Environmental Engineering, University of Alberta, Edmonton, Alberta

ABSTRACT
A field and laboratory research program was performed to examine the mechanisms leading to the rapid densification of the mature fine tailings (MFT) in Syncrude's Mildred Lake Settling Basin (MLSB) during microbial activity. This paper will describe the new laboratory apparatus used to test the consolidation and biochemical properties of the MFT during microbial activity. The complete outline of the laboratory testing program will be highlighted but because of space limitations only the detailed results for one series of tests will described in the paper. Preliminary discussion on the primary geotechnical mechanisms leading to the rapid densification of the MFT due to microbial activity is provided.

RÉSUMÉ
Un programme de recherche de terrain et de laboratoire a été accompli pour examiner les mécanismes causant densification rapide de tailings parfait adulte (MFT) à Mildred Lake du Syncrude Installant la cuvette (MLSB) pendant l'activité microbienne. Ce papier décrira le nouvel appareil de laboratoire utilisé pour évaluer la consolidation et les propriétés biochimiques du MFT pendant l'activité microbienne. Le contour complet du programme de mise à l'essai de laboratoire sera accentué mais seulement les résultats détaillés pour une série d'épreuves iront faire décrit dans le papier (essentiellement en raison des restrictions spatiales). La discussion préliminaire sur les mécanismes geotechnical primaires causant densification rapide de MFT en raison de l'activité microbienne est fournie..

1 INTRODUCTION

In the oil sands industry, bitumen is extracted by the Clark hot water extraction method. After extraction, the bitumen is sent to an upgrading plant for further processing while the waste material, including mineral particles, water, and residual bitumen, is discharged into large tailings ponds. The mineral particles consist of sand (particle size > 44um), and fines (<44um). The coarse sand particles rapidly settle to form dykes or beaches, however the fines particles settle slowly. It takes 2 to 3 years to reach about 30% solids content and is then called mature fine tailings (MFT). Due to the large depth and very low permeability, the densification under self-weight is very slow and it is estimated that it will take more than 100 years to become trafficable under natural conditions. The MLSB is the largest tailings pond for MFT storage at Syncrude. Started in 1978 it now contains more than 200 Mm^3 of MFT and capping water with a surface area of about 11 km^2 and a maximum depth of more than 50 m. The MFT densification was very slow until the occurrence of intense microbial activity in the mid 1990s. Figure 1 shows the location of the MLSB with 3 sites used to monitor the tailings behavior for over 20 years. Figure 2 shows gas bubbles on the pond surface and Figure 3 shows a densified sample with gas voids at Site 1 in 2002. Historical monitoring data and field investigations have identified the rapid densification phenomenon and its connection with biogas generation (Guo, et.al., 2002). Laboratory small scale column tests have preliminarily modeled the rapid densification of the MFT with microbial activity (Guo, et. al, 2004). However, the in-depth mechanism is still unclear. A new test apparatus was developed to model the MFT densification under microbial activity. Gas MFT densification tests (both geotechnical and chemical tests) were carried out at the University of Alberta to study the mechanism of the rapid densification

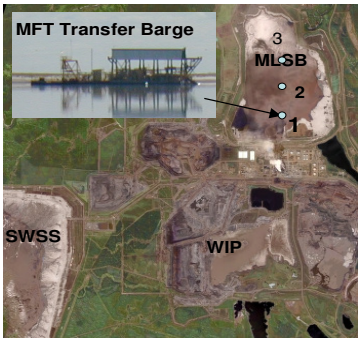

Figure 1 Syncrude's MLSB and three monitoring sites


Figure 2 Gas bubbles on the surface of the south part of the pond in 2002

phenomenon. This paper describes the test apparatus, the test program, and the test results of a sequence of tests. The mechanism of the rapid densification of this sequence is analyzed.

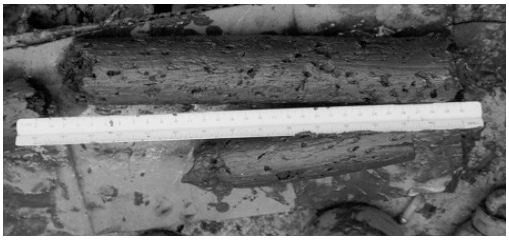

Figure 3 A densified MFT sample at Site 1 in 2002

2 TEST APPARATUS

As shown in Figure 4, the test apparatus consists of an acrylic cell of 15 cm inner diameter, an acrylic gas cylinder (released gas cylinder) with an inner diameter of 1.92 cm or 3.809 cm, depending on expected gas volume, and a water collection standpipe with an inner diameter 1.11 cm. A plastic tube, 0.42 cm inner diameter, connects the test cell to the standpipe where the drained water is collected and measured during biogas generation. A submergible LVDT (Linear Variable Differential Transformer) was used to accurately measure the water-MFT interface movement. Three differential pressure transducers (T1, T2, T3) were used to measure the pore water pressures at different elevations (E1, E2, E3) in the sample. Transducer T4 was used to measure the hydrostatic changes in the test cell. Released gas thicknesses in the headspace were measured visually using a ruler taped on the outside wall of the gas cylinder. Water front movement in the plastic tube was also measured by visual observations.

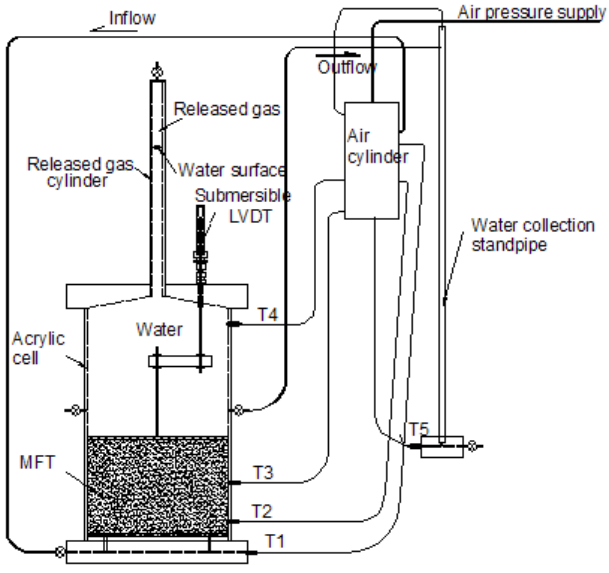

Figure 4 Schematic sketch of gas MFT densification test

At the beginning of the test, the space above the water-MFT interface was filled with pond water before microbial activity was initiated by raising the room temperature from 4°C to about 24°C. Due to biogas generation, water in the test cell was partly pushed out into the water collection standpipe through the plastic tube. Water volumes in the water collection standpipe were measured using the pressure measurements from transducer T5.

In order to model biological activities at different depths of the pond, different air pressures, 0 and 60 kPa, were applied to the test system by a stable air pressure supply. An air cylinder, shown in Figure 4, was used to apply back pressure to the whole test system, including the test cell, released gas cylinder, water collection standpipe and the external ports of all differential pressure transducers, using a series of small plastic tubes. The pressure in the air pressure cylinder was controlled using a low-pressure regulator. When the air cylinder was open to the atmosphere, the gas MFT densification tests were carried out without air pressure being applied. The samples were incubated at about 24°C during microbial activity. When gas accumulation in the MFT reached a critical value, part of the generated gas released to the headspace of the gas cylinder.

Before and after microbial activity, the room temperature was lowered to 4°C to inhibit microbial activity. At this room temperature, hydraulic conductivity tests were conducted to measure the coefficients of permeability. Constant head differences were applied by fixing the inflow tube (connected with a valve at the bottom of the cell) above the outflow tube to cause upward flow, as illustrated in Figure 4.

Two types of tests, gas MFT densification tests and chemical sampling tests were conducted. Sub-samples were taken from the chemical cells to study the chemical and microbiological properties of the MFT during microbial activity. The apparatus for the chemical tests was similar to that of the gas MFT densification tests, as shown in Figure 4, except that pore water pressure changes and interface movements were not monitored in the chemical sampling tests.

3 TEST PROCEDURE AND PROGRAM

The laboratory bio-densification tests were carried out from October 2003 to October 2004, with three sequences as shown in Table 1. Sequence 1 conducted first and Sequence 2 and Sequence 3 followed. A total of 27 tests were conducted: 18 densification tests and 9 chemical sampling tests. These tests were used to model the bio-densification properties of the MFT under different conditions (microbial activity intensity, stress history, and depth in the pond). Different amounts of sodium acetate, 0, 0.6 and 1.75 g/L of MFT, were added to the samples before testing. Samples 1 to 6 and 7© to 9© (chemical sampling tests) were self-weight consolidated at 4 degree temperature before microbial activity was initiated. They

Table 1 Overview of gas MFT densification tests

Sequence No	1			2			3			Sodium Acetate (g/L)
Test No	1	4	7©	10	13	16©	19	22	25©	0
	2	5	8©	11	14	17©	20	23	26©	0.6
	3	6	9©	12	15	18©	21	24	27©	1.75
Air Pressure (kPa)	0	60	0	0	0	0	0	60	60	

Table 2 Some initial parameters of Samples 13 to 15 before microbial activity

Solids Content (%)	Void Ratio (e)	Density (g/ml)	Water Content (%)	Bitumen Content (%)
34.5	4.3	1.237	189.9	4.29

represent the normally consolidated MFT under self-weight. Samples 19 to 24 and Samples 25© to 27© (chemical sampling tests) were consolidated under 1.0 kPa loading before microbial activity. They represent the normally consolidated MFT under an external loading. Tests 10 to 12 were similar to Tests 19 to 24, but, after the 1.0 kPa consolidation was finished, the loads on Samples 10 to 12 were released, and the microbial activities started. These three tests were used to model the stress condition of over-consolidated MFT. For Tests 13 to 15 and Tests 16© to 18©, microbial activities were stimulated shortly after the MFT was poured into the cells. They represent the soft MFT without pre-consolidation, a condition similar to the MFT at the MLSB before microbial activity initiation. The results of these six tests are presented in this paper.

During microbial activity, 60 kPa air pressure was applied to Samples 4 to 6, 22 to 24, and 25© to 27© to model microbial activities at certain depths of the pond. For all other samples, microbial activities were under atmospheric pressure plus about 1.0 m water head. The overall procedure of the gas MFT densification tests can be summarized as follows:

- Sample preparation and initial parameter measurements.
- Consolidation under self-weight (Samples 1 to 6) or 1.0 kPa loading (Samples 10 to 12 and Samples 19 to 24) at 4°C temperature.
- After 1.0 kPa consolidation, the loads on Samples 10 to 12 were released.
- Permeability test at 4°C, except for Tests 13 to 15 and Tests 16© to 18©
- Microbial activity and biogas generation at 24°C.
- Permeability test again at 4°C.

Tests 1 to 6 and 7© to 9© comprised the first sequence (biogas generation from Oct. 30 to Dec. 24, 2003), Tests 10 to 15 and 16© to 18© comprised the second sequence (biogas generation from Dec.24, 2003 to Feb. 12, 2004) and Tests 19 to 24 and 25© to 27© were the final sequence (biogas generation from June 15 to Oct. 8, 2004). The complete test program lasted approximately 12 months. The tests (including consolidation and gas MFT densification tests) were carried out in a temperature-controlled cool room. Some experimental results were determined from the measurements by LVDT, pressure transducers, and visual observations. The estimation of volumetric changes (like water volume, gas volume, solids volume) in the MFT samples is based on water mass balance in the whole test system. Some volumetric parameters like water void ratio, gas void ratio, degree of saturation, gas content, etc., could then be calculated.

From the volumetric changes and pore water pressure measurements, the total stress and pore water pressure in the MFT sample can be obtained. The concept of "operative stress" (Sills et al., 1991) is introduced to interpret rapid densification of the MFT during microbial activity. The operative stress is defined as:

$$\sigma_{op} = \sigma - u \qquad [1]$$

where, σ_{op} is operative stress, σ is total stress, and u is pore water pressure.

It is considered that the "operative stress" concept is applicable for soils with occluded gas bubbles, and that for any initial gas content, water void ratio (e_w) is controlled by operative stress (Sills et al., 1991).

4 TESTS 13 to 15 RESULTS

Table 2 shows the initial parameters of the MFT material in Samples 13 to 15. The initial properties of the three samples were similar. The test cells were flushed with nitrogen gas to create an anaerobic environment. Then, the mixed samples were poured into the test cells to a height of 8.2 cm. The densification test apparatus, as shown in Figure 4, was then assembled. Without pre-consolidation and permeability tests, the room temperature was raised to 24°C to start microbial activity.

Figure 5 shows the changes of total gas volume (trapped gas plus released gas) and released gas volume during microbial activity at STP (standard temperature, 25°c and pressure 1 atm.). There was no obvious gas generation in Sample 13 during the first 100 hours. It is likely that any generated gas was dissolved in the pore water and bitumen during this period. After 100 hours, gas was generated at a slow rate. In Sample 14, the total gas volume increased slowly during the first 80 hours, after which time the gas generation rate accelerated. After about 340 hours, microbial activity in Sample 14 diminished and the total gas generation volume became stable. In Sample 15, gas was generated at slow rates during the first 100 hours. From 100 to 200 hours, gas

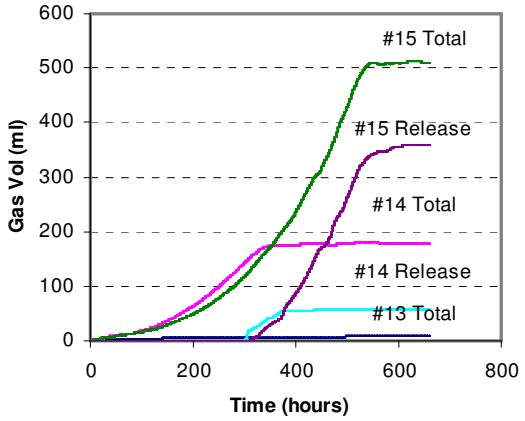

Figure 5 Total and released gas volumes with time

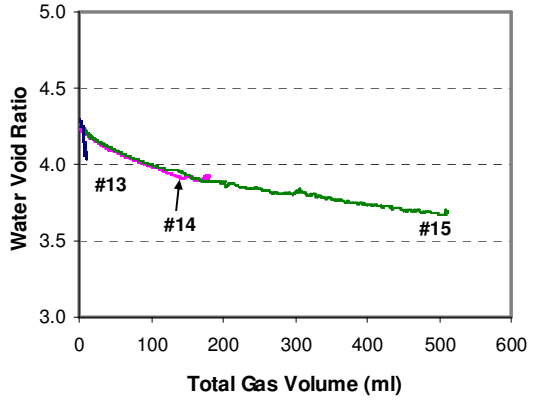

Figure 6 Water void ratio vs. total gas volume (STP) in Samples 13-15

generation rates gradually increased. From 200 to 550 hours, gas was generated very rapidly. After about 550 hours, microbial activity in Sample 15 diminished and the total gas volume became stable. At the end of testing, the total gas volumes (at STP) in Samples 13 to 15 were 9 mL, 179 mL and 510 mL, respectively. In Sample 13, all the generated gas was trapped. In Samples 14 and 15, gas bubbles started to be released after about 300 hours. At the end of testing, the released gas volumes from Samples 14 and 15 were 58 mL and 358 mL, respectively.

Figure 6 shows total generated gas volume vs. water void ratio for Samples 13 to 15. When the total gas generation volume increased, more water drained out of the MFT samples. At the end of testing, the water void ratios of Samples 13 to 15 were 4.04, 3.91 and 3.68, respectively. Due to very slow gas generation, water drainage from Sample 13 was less affected by microbial activity (Sample 13 was similar to a saturated soil).Tests 14 and 15 had intense biogas generation. The curves for the two tests almost merged as a single one. This indicates the water drainage rate is controlled by the biogas generation rate during intense microbial activity.

Figures 7 and 8 show the volumetric changes (trapped gas volume, released gas volume and total gas volume at STP, and water drainage volume) of Samples 13 and 15, respectively. The changes of Sample 14 were similar to those of Sample 15. Gas was generated very slowly with no gas releasing in Sample 13, and correspondingly, water drained out of the MFT slowly. Water drained out of Sample 15 at relatively slow rates during the first 160 hours due to slow gas generation. As the gas generation accelerated, the water drainage rate increased. After about 550 hours, with biogas generation diminishing, the

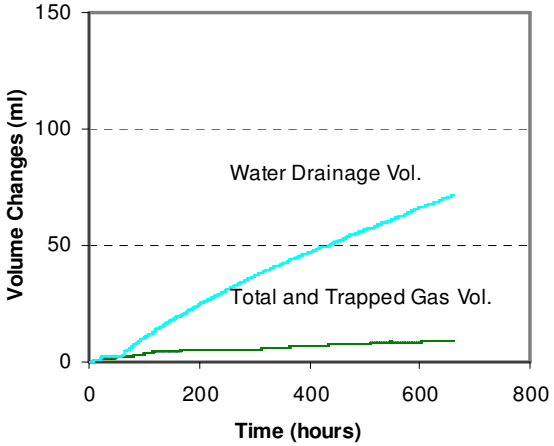

Figure 7 Volumetric changes in Sample 13 during microbial activity

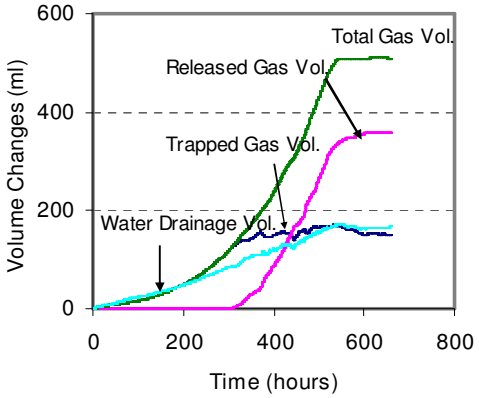

Figure 8 Volumetric changes in Sample 15 during microbial activity

water drainage volume from Sample 15 became stable. During intense microbial activity, water drainage rates were significantly affected by gas generation rates.

Figure 9 shows the changes of the bulk density with time during microbial activity. The bulk density of Sample 13 slightly increased from 1.237 to 1.241g/mL with slow gas generation. With the increases of trapped gas volume in Samples 14 and 15, the bulk densities decreased with time. When the trapped gas volume became stable, the bulk density showed less change. At the end of testing, the bulk densities of Samples 13 to 15 were 1.24 g/mL, 1.16 g/mL and 1.15 g/mL, respectively. At the end of testing, the degree of saturation of Sample 13 was about 99%. The values of the degree of saturation of samples 14 and 15 were 91% and 88%, respectively.

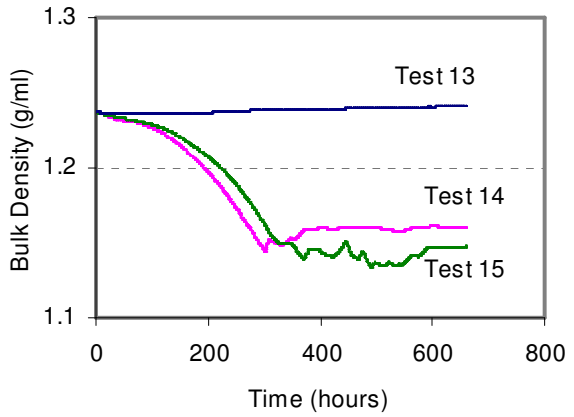

Figure 9 Bulk density vs. time in Samples 13 to 15

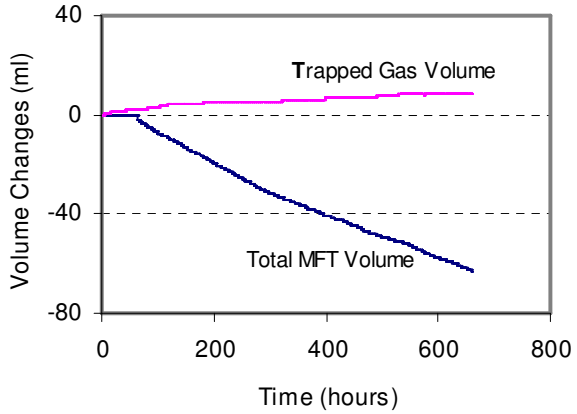

Figure 10 Changes in trapped gas volume and total MFT volume (STP) in Sample 13

Figures 10 and 11 show the changes of the trapped gas volume and total MFT volume with time in Samples 13 and 15, respectively. The slow gas generation in Sample 13 had little effect on the MFT behavior. The sample was similar to saturated soil. During testing, the trapped gas volume increased very slowly and the total MFT volume slowly decreased. In Sample 15, the trapped gas volume slowly increased with time during the first 160 hours, but the total MFT volume slightly decreased or stabilized. From 160 hours to 320 hours, the trapped gas volume rapidly increased with time, but the MFT volume expansion lagged far behind the increase of the trapped gas volume. As a result, part of the space required by trapped gas bubbles was obtained by pushing water out of the sample. After 320 hours, gas started to be released from Sample 15. The trapped gas volume slowly increased with time or stabilized, but the global MFT volume rapidly decreased due to a structural collapse during gas bubble release. More water was rapidly drained out of Sample 15.

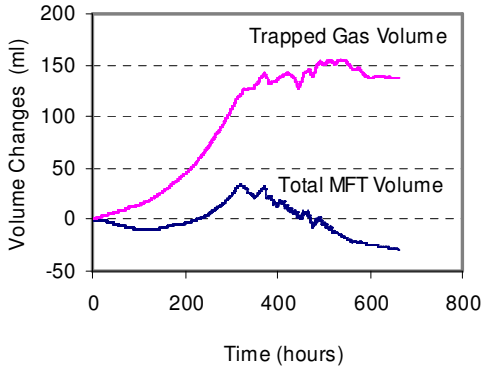

Figure 11 Changes in trapped gas volume and total MFT volume (STP) in Sample 15

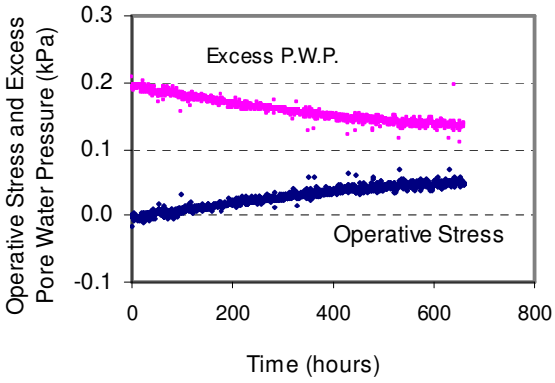

Figure 12 Changes in excess pore pressure and operative stress at E1 of Test 13

Figure 12 shows the changes of excess pore water pressure and operative stress at the bottom (E1) of Sample 13 during microbial activity. Due to very slow biogas generation, the bulk density of the sample had only slight changes as shown in Figure 9. The total stress in the sample was relatively stable. During the first 24 hours, due to a rapid temperature increase, excess pore water pressure slightly increased and operative stress slightly decreased. From 24 hours to the end of testing (660 hours), excess pore water pressure slowly

decreased, and operative stress slowly increased. The behavior of Sample 13 was similar to a saturated soft soil.

Figures 13 and 14 show the changes of excess pore water pressure and operative stress, respectively, at the bottom (E1) of Sample 15. During the first 320 hours, the bulk density of the sample and total stress decreased due to the increase of the trapped gas volume in the MFT and water being expelled out of the test cell. From 0 to 100 hours, gas was generated at slow rates, excess pore water pressure slowly decreased and operative stress slowly increased. From 100 to 160 hours, biogas generation gradually accelerated and the trapped gas volume increased with time. Excess pore water pressure slightly increased, and operative stress decreased within this time frame. From 160 to 320 hours, the trapped gas volume rapidly increased in the MFT and the total stress noticeably decreased. There was rapid water drainage from the MFT during this period. Due to a decrease in total stress the excess pore water pressure decreased but the operative stress had only a slight increase. It is not appropriate to compare the operative stress changes as the total stress was not constant. An obvious increase in operative stress would have been anticipated if the total stress were constant. This was proven by the subsequent

Table 3 Some parameters of Samples 13 to 15 after microbial activity

Test No	Solids Content (%	Density (g/ml)	Water Void Ratio	Gas Void Ratio	Total Void Ratio	Degree of Saturation (%)
13	35.8	1.241	4.04	0.031	4.07	99.2
14	36.4	1.161	3.91	0.38	4.29	91.1
15	37.9	1.147	3.68	0.48	4.16	88.5

Table 4 Coefficients of permeability of Samples 13 to 15 after microbial activity

Test No	13	14	15
Coefficient of permeability (10^{-9} m/s)	7.29	13.8	19.64

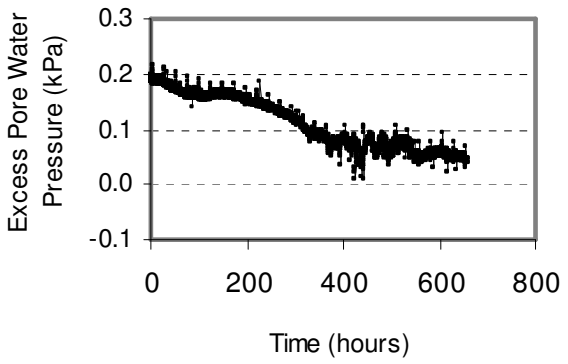

Figure 13 Changes in excess pore pressure at E1 of Test 15

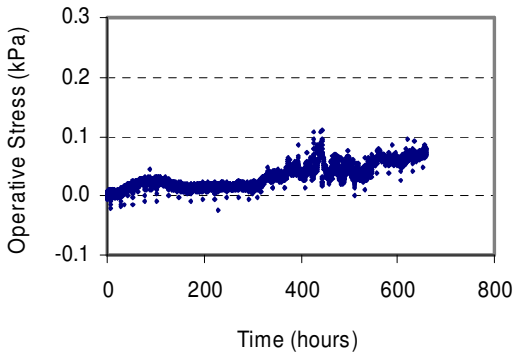

Figure 14 Changes in operative stress at E1 of Test 15

period of microbial activity. From 320 hours to 550 hours, gas was intensely released from the MFT and the excess pore water pressure decreased and the operative stress increased. The trapped gas volume, bulk density, and the total stress were relatively stable. After 550 hours, with microbial activity diminishing, both excess pore water pressure and operative stress became stable and water drainage from the MFT became very slow.

Table 3 shows some parameters of Samples 13 to 15 after microbial activity. Sample 15 had the highest gas void ratio but the lowest water void ratio. After the microbial activity diminished in the three samples, the room temperature was lowered to about 4°C to further inhibit the microbial activity and constant head permeability tests were conducted. Table 4 summarizes the test results. The coefficients of permeability in Samples 14 and 15 were higher than the value of Sample 13. It's likely some fractures or gas release voids became drainage paths.

At the end of testing, a small copper tube was inserted into Samples 13 to 15 and nitrogen gas with a temperature of –70°C was introduced into the tube to freeze the nearby MFT. After about five minutes, a cylindrical zone of about 1 to 2 cm was frozen around the tube. Because the freezing operation was conducted carefully, the MFT structure was well preserved. The frozen samples were used to analyze the structural properties of the MFT. The tests were conducted at the Scanning Electron Microscope (SEM) Laboratory at the Department of Earth and Atmospheric Science, University of Alberta. The Cryo-electron Microscopy method (Al-Amoudi, et. al., 2004) was used during analysis.

Figure 15 shows the SEM images of Samples 13 and 15 after microbial activity. In Sample 13, a typical dispersed structure was observed; the particles or particle domains (in white color, a group of particles with close face-face contacts) were parallel to each other with large spaces (mainly filled with water) in between. This image reflects high water content within clay particles. The net repulsive force between the particles causes the meta-stable face-to-face arrangements (Craig, 1993). With respect to Sample 13, more edge-to-face and edge-to-edge contacts

and relatively lower water content are shown in Sample 15 image. This was likely due to the collapse of the initial dispersed structure and rapid dewatering during intense biogas activity.

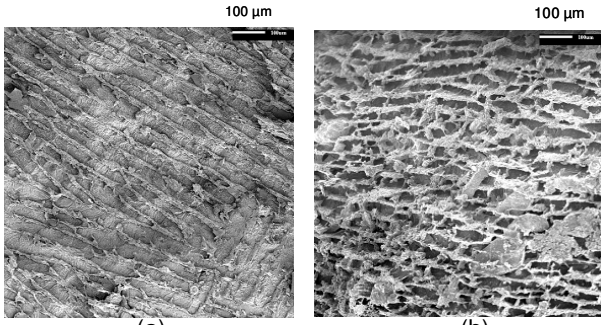

(a) (b)

Figure 15 SEM images of Samples 13 (a) and 15 (b) after microbial activity

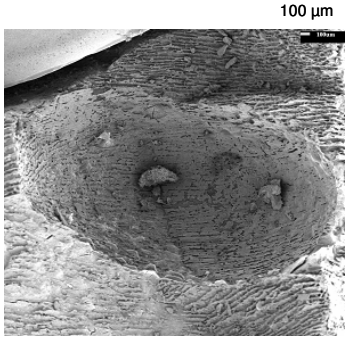

Figure 16 A large gas bubble in Sample 14

Figure 16 shows a large gas bubble and a thin membrane of clay on the sidewall of the gas void. Within the membrane, the clay particles were re-oriented with faces parallel to the wall. It appears that the clay particles surrounding the gas bubble were compressed and re-oriented during gas bubble formation

5 RESULTS for CHEMICAL TESTS 16©, 17©, and 18©

Tests 16© to 18© were duplicate tests of Samples 13 to 15, respectively. They were used to sacrificially get samples for chemical and microbiological measurements during microbial activity. A plastic piston syringe connected with a hollow copper tube of small diameter was used as the sampler. When sampling, a small copper tube was inserted into the cell through a valve mounted 1.45 cm above the bottom of the sample. By pulling back the piston of the syringe, the MFT slurry was sucked into the sampler. The samples were then ejected into glass jars and sealed.

Chemical measurements were performed at the Syncrude Edmonton Research Centre using standard industry methods (Syncrude, 1995). The analyses included pH, EC, alkalinity, cations, anions, and selected trace elements. In this research, some parameters, including pH, EC, and the concentrations of some ions (Na^+, K^+, Ca^{2+}, Mg^{2+}, SO_4^{2-}, Cl^-, HCO_3^-), were analyzed. The detailed chemical changes are not shown here due to space restriction, but some results are briefly summarized. During microbial activity, acetate concentrations decreased with time and were completely depleted at the end of testing. The pH values slightly increased from 7.4 to 7.5 at the start of testing to 7.7 to 7.8 by the end of microbial activity. SO_4^{2-} concentrations decreased from 46 mg/L to below 10 mg/L after microbial activity. Cl^- concentrations were relatively stable, HCO_3^- concentrations decreased with time. During microbial activity, the concentrations of the cations (Na^+, K^+, Ca^{2+}, Mg^{2+}) decreased with time. The values of Electrical Conductivity also decreased with time in the three samples. The chemical changes in Test 18© were more obvious than those in Tests 16© and 17©.

6 MPNs of METHANOGEN and SULFATE-REDUCING BACTERIA (SRB)

Methanogens and Sulfate-reducing Bacteria (SRB) are two important microorganisms active in the MLSB (Sobolewski, 1992). They compete with each other for energy sources. For a given substrate, SRB obtain more energy than do methanogens, so they out-compete the latter for the substrate if sulfate is abundant (Fedorak et al., 2002). It has been found that methanogenesis at the MLSB became significant only after the sulfate concentrations dropped (Holowenko et al., 2000).

During the tests, samples were obtained for chemical and microbiological measurements. Small amounts (about 5 mL) of the samples in the plastic syringe were ejected into glass tubes for enumerations of methanogens and SRB. These glass tubes were flushed with nitrogen gas to create an anaerobic environment prior to sampling. Microbiological enumeration tests were performed using the standard five-tube Most Probable Number (MPN) method, with serial 10-fold dilutions of the MFT samples **(**Fedorak et al., 2002).

During testing, three samples were obtained at different times from each sample. The first sampling was conducted at 4°C before microbial activity was initiated. The second sampling was conducted on the eighth day of microbial activity at 24°C temperature. The third sampling was conducted at the end of testing at 4°C. During the tests, the methanogen MPN values of Samples 16© to 18© ranged from 10^2 to 10^3 MPN/mL, and the SRB MPN values ranged from 10^4 to 10^5 MPN/mL. There were no significant changes in both MPN values during microbial activity. Some fluctuations were probably due to material heterogeneity, sampling or testing errors.

During gas MFT densification tests, the released gas in the headspace was collected in a Tedlar bag and

analyzed by Gas Chromatography (GC). These tests were conducted in the Environmental Engineering Laboratory at the University of Alberta. Luo (2004) has given a detailed description about the test mechanism, equipment, operation and calibration used. Table 5 shows the percentages of some major gas components in the headspaces of Cells 17© and 18©. In Cell 18©, the methane accounted for more than 80% of the released gas in the headspace. This indicates that methanogenesis was the dominant microbial activity during the test. Trace amounts of O_2 (0.07%) found likely came from the atmosphere during sampling or GC testing. Small amounts of CO_2 (1.24%) were detected. In the Tedlar bag of Cell 17©, N_2 was the major gas, and the measured O_2 gas content was 11.5%. Since the released gas volume in headspace of Cell 17© and the volume of methane gas collected in the Tedlar bag were small, the results of the GC analyses were greatly affected by environmental gases (gases in the air or nitrogen gas when flushing the Tedlar bag). Some gases such as H_2S were not detected by the equipment. It's likely that the concentrations of these gases were relatively small and the device was not sensitive enough to detect them.

Table 5 Results of GC analyses of the released gas from Tests 17© and 18©

Test No.	CH4 (%)	N2 (%)	O2 (%)	CO2 (%)
17©	23.4	66.8	11.5	0.17
18©	80.8	2.22	0.07	1.24

7 CONCLUSIONS

From the results of Tests 13 to 15 and 16© to 18©, some conclusions can be summarized as follows:

- Gas MFT densification tests have confirmed that, water drainage rates were related to gas generation rates during intense biogas generation;
- During rapid gas generation, the total MFT volume increase lagged behind the trapped gas volume due to structural resistance, so water was rapidly pushed out of the MFT;
- During rapid gas release, the MFT structure evidently collapsed, total MFT volume decreased more rapidly than trapped gas volume and more water rapidly drained out;
- During intense gas generation and release, the operative stress changes were complex due to total stress changes. When the total stress became stable, the operative stress obviously increased while water drained out rapidly.
- After intense biogas generation, the MFT structure became denser and more aggregated, and the coefficients of permeability increased.
- The paper only presents Tests 13 to 15 and 16© to 18©. The results were significantly different for tests under different conditions (stress history, total stress, etc). These results will be presented in the future.

8 ACKNOWLEDGEMENTS

The authors would like to acknowledge the financial and technical support provided by Syncrude Canada Ltd., Suncor Energy Inc., and Canadian Natural Resource Ltd. We also appreciate the advice and support of Dr. Mike MacKinnon, formally with Syncrude Canada Ltd..

9 REFERENCES

Al-Amoudi, A., Norlen, L.P., Doborchet, J., 2004. Cryo-electron microscopy of vitreous sections of native biological cells and tissues. Journal of Structural Biology, 148 (1):131-5.

Craig, R.F. 1992. Soil Mechanics, the fifth edition, Chapman & Hall, London, UK.

Fedorak P.M., Coy D.L., Salloum M.J., and Dudas M.J., 2002. Methanogenic potential of tailings samples from oil sands extraction plants. Can. J. Microbiol. 48: 21-33.

Guo, C., Chalaturnyk, R.J., Scott, J.D., MacKinnon, M., and Cyre, G., 2002. Geotechnical field investigation of the densification phenomenon in the oil sands mature fine tailings. 55th Canadian Geotechnical Conference, Niagara Falls, Ontario, 8 pages on a CD.

Guo, C., Chalaturnyk, R.J., Scott, J.D., MacKinnon, M., 2004. Densification of oil sands tailings by biological gas generation. 57th Canadian Geotechnical Conference, Quebec City, 8 pages on a CD.

Holowenko, F.M., MacKinnon, M.D., and Fedorak, P.M. 2000. Methanogens and surfate-reducing bacteria in oil sand fine tailings wastes. Can. J. Microbial 46:927-937.

Luo, G.X., 2004. Investigation of CT Beneath MFT Deposition for Oil Sands Tailings Disposal. M.Sc thesis, Department of Civil and Environmental Engineering, University of Alberta, Edmonton, AB, Canada.

Sobolewski, A. 1992. The microbial characteristics of oil sands tailings sludge. Consultant's report submitted to Alberta Oil Sands Technology Research Authority. Calgary, Alberta.

Sills, G.C., Wheeler, S.J., Thomas, S.D., and Gardner, T.N., 1991. Behaviour of offshore soils containing gas bubbles. Geotechnique 41, No. 2, 227-241.

Syncrude Canada Ltd. 1995. Syncrude Analytical Methods (SAM) Manual. 4th ed. Syncrude Canada Ltd. Research Department. Edmonton, Alberta.